THE BUILDUP OF THE RED SEQUENCE IN GALAXY CLUSTERS SINCE $z \sim 0.8$[1]

G. De Lucia,[2] B. M. Poggianti,[3] A. Aragón-Salamanca,[4] D. Clowe,[5] C. Halliday,[3] P. Jablonka,[6] B. Milvang-Jensen,[7]
R. Pelló,[8] S. Poirier,[6] G. Rudnick,[2] R. Saglia,[7] L. Simard,[9] AND S. D. M. White[2]

ABSTRACT

We study the rest-frame $(U - V)$ color-magnitude relation in four clusters at redshifts 0.7–0.8, drawn from the ESO Distant Cluster Survey (EDisCS). We confirm that the red-sequence galaxies in these clusters can be described as an old, passively evolving population, and we demonstrate that, by comparison with the Coma Cluster, there has been significant evolution in the stellar mass distribution of red-sequence galaxies since $z \sim 0.75$. The EDisCS clusters exhibit a deficiency of low-luminosity passive red galaxies. Defining as "faint" all galaxies in the passive evolution–corrected range $0.4 \gtrsim L/L_* \gtrsim 0.1$, the luminous-to-faint ratio of red-sequence galaxies varies from 0.34 ± 0.06 for the Coma Cluster to 0.81 ± 0.18 for the high-redshift clusters. These results exclude a synchronous formation of all red-sequence galaxies and suggest that a large fraction of the faint red galaxies in current clusters moved on to the red sequence relatively recently. Their star formation activity presumably came to an end at $z \lesssim 0.8$.

Subject headings: galaxies: clusters: general — galaxies: elliptical and lenticular, cD — galaxies: evolution — galaxies: formation

1. INTRODUCTION

It has long been known (Visvanathan & Sandage 1977) that red cluster galaxies form a tight sequence in the color-magnitude (CM) diagram that, in nearby clusters, extends at least 5–6 mag fainter than the Brightest Cluster Galaxy (BCG; De Propris et al. 1998). The existence of a tight color-magnitude relation (CMR) for early-type cluster galaxies up to a redshift of ~1 and the evolution of its slope and its zero point as a function of redshift are commonly interpreted as the result of a formation scenario in which cluster elliptical galaxies constitute a passively evolving population formed at high redshift ($z \gtrsim 2$–3; Ellis et al. 1997; Stanford et al. 1998; Gladders et al. 1998). In this model, the slope of the relation reflects metallicity differences and naturally arises through the effects of supernova winds (Kodama et al. 1998). An alternative explanation has been proposed by Kauffmann & Charlot (1998; see also De Lucia et al. 2004). In this model, elliptical galaxies form through mergers of disk systems, and a CMR arises as a result of the fact that more massive elliptical galaxies are formed by mergers of more massive, and hence more metal-rich, disk systems.

The homogeneity of cluster elliptical galaxies should, however, be contrasted with the increasing observational evidence that red passive galaxies in distant clusters constitute only a

subset of the passive galaxy population in clusters today (van Dokkum & Franx 1996). Distant clusters contain significant populations of galaxies with active star formation that must have eventually evolved on to the CM sequence after their star formation activity was terminated, possibly as a consequence of their environment (Smail et al. 1998; Dressler et al. 1999; Poggianti et al. 1999).

In this Letter we present the CMR for four clusters in the redshift interval 0.7–0.8 from the ESO Distant Cluster Survey (EDisCS). In the following, we use $\Omega_m = 0.3$, $\Omega_\Lambda = 0.7$, and $H_0 = 70$ km s^{-1} Mpc^{-1}.

2. THE DATA

The EDisCS is an ESO Large Programme aimed at the study of cluster structure and cluster galaxy evolution over a significant fraction of cosmic time. The complete EDisCS data set provides homogeneous photometry and spectroscopy for 10 clusters at redshift 0.4–0.5 and 10 clusters at redshift 0.6–0.8. In this Letter we present results for four clusters at redshift 0.7 (Cl 1040.7−1155 and Cl 1054.4−1146), 0.75 (Cl 1054.7−1245), and 0.8 (Cl 1216.8−1201).

The clusters used in this analysis have been imaged in V, R, and I with FORS2 ($6'.8 \times 6'.8$) on the ESO Very Large Telescope (VLT). The average integration times used were 115 m in the I band and 120 m in the V band. Multiobject spectroscopy was carried out using FORS2 on VLT. The clusters in the high-redshift sample (which includes those used in this study) have also been imaged in J and K (SOFI-NTT, $5'.5 \times 5'.5$). A brief description of the cluster sample selection is given in Rudnick et al. (2003). All data and details about their analysis will be presented in forthcoming papers (S. D. M. White et al. 2004, in preparation; C. Halliday et al. 2004, in preparation; A. Aragón-Salamanca et al. 2004, in preparation). The number of spectroscopically confirmed members for the clusters presented in this analysis ranges from 30 (Cl 1040.7−1155) to 70 (Cl 1216.9−1136).

Object catalogs have been created using the SExtractor software (Bertin & Arnouts 1996) in "two-image" mode, using the I-band images as detection reference images. In the following, we will use magnitudes and colors measured on the seeing-

[2] Max-Planck-Institut für Astrophysik, Karl-Schwarzschild-Strasse 1, Postfach 1317, D-85748 Garching bei München, Germany.

[3] Osservatorio Astronomico di Padova, Vicolo dell'Osservatorio 5, I-35122 Padua, Italy.

[4] School of Physics and Astronomy, University of Nottingham, NG7 2RD, UK.

[5] Steward Observatory, University of Arizona, 933 North Cherry Avenue, Tucson, AZ 85721.

[6] Observatoire de Paris, 5 Place Jules Janssen, F-92195 Meudon Cedex, France.

[7] Max-Planck-Institut für extraterrestrische Physik, Giessenbachstrasse, Postfach 1312, D-85748 Garching, Germany.

[8] Laboratoire d'Astrophysique, UMR 5572, Observatoire Midi-Pyrénées, 14 Avenue Edouard Belin, F-31400 Toulouse, France.

[9] Herzberg Institute of Astrophysics, National Research Council of Canada, 5071 West Saanich Road, Victoria, BC V9E 2E7, Canada.

matched (to 0″.8—our "worst" seeing) registered frames using a fixed circular aperture with 1″.0 radius. At the clusters' redshifts, this corresponds to a physical radius of 7.13–7.50 kpc. This choice has been adopted in order to simplify the comparison with the Coma Cluster (see § 4).

3. CLUSTER MEMBERSHIP

Photometric redshifts were computed using two independent codes (Rudnick et al. 2001; Bolzonella et al. 2000) to better keep under control systematics in the identification of likely nonmembers. A detailed analysis of the performance of both codes on EDisCS data will be presented in a separate paper (R. Pelló et al. 2004, in preparation). Results based on the current spectroscopic sample show that our photometric redshifts are quite accurate, with $\langle |z_{spec} - z_{phot}| \rangle = 0.06$–$0.08$. Unless otherwise stated, nonmembers are rejected in the following using a two-step procedure: (1) the full redshift probability distributions from both codes are used to reject objects with low probability of being at the cluster redshift (e.g., Brunner & Lubin 2000), and (2) a statistical subtraction is performed on the remaining objects using the distribution on the CM diagram of all the objects at a physical distance from the BCG larger than 1 Mpc (Kodama & Bower 2001). Our photometric redshift selection rejects 85%–90% of the objects in the original photometric catalogs (containing 2600–3100 objects, down to a magnitude limit of 25 in the I band); 40%–50% of the remaining objects are subtracted statistically.

4. THE COLOR-MAGNITUDE RELATION

Figure 1 shows the $V - I$ diagram for the four clusters used in this analysis. At the clusters' redshifts, $V - I$ approximately samples the rest-frame $U - V$ color, which straddles the 4000 Å Balmer break and is therefore very sensitive to any recent or ongoing star formation (SF). A red sequence is clearly visible in the CM diagram of each cluster, together with a significant population of the blue galaxies known to populate high-redshifts clusters.

The filled squares and diamonds in Figure 1 show the locations of galaxy models with two different SF histories: a single burst at $z = 3$ (*diamonds*) and an exponentially declining SF starting at $z = 3$ (*squares*) with $\tau = 1$ Gyr. Both were calculated with the population synthesis code by Bruzual & Charlot (2003). For each SF history, three different metallicities are shown: 0.02, 0.008, and 0.004, going from brighter to fainter objects. The relation between metallicity and luminosity in these models has been calibrated by requiring that they reproduce the observed CMR in Coma,[10] as shown in Figure 2. Here we use the data from Terlevich et al. (2001), and we use their magnitudes and colors in a 25″.2 diameter aperture. At the redshift of Coma, this corresponds to a physical size of 11.71 kpc, quite closely approximating our ~14 kpc aperture at $z \sim 0.8$. Figure 1 shows that the single-burst model provides a remarkably good fit to the red sequence observed in the high-redshift clusters, confirming that the location of the CM sequence observed in distant clusters requires high redshifts of formation and that the slope is consistent with a correlation between galaxy metal content and luminosity.

[10] This calibration has been found a posteriori to be in good agreement with the metallicity-luminosity relation derived from spectral indices of Coma galaxies (Poggianti et al. 2001).
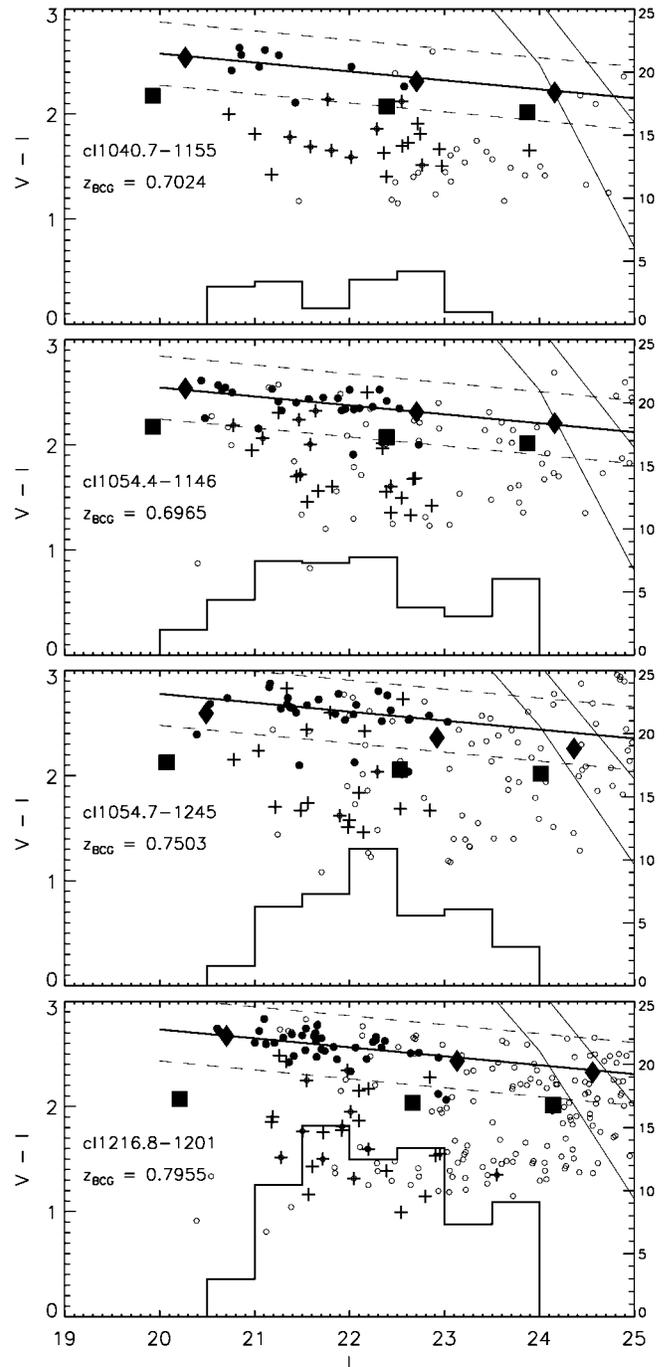
FIG. 1.—CM diagrams for the four clusters under investigation. The thick solid line represents the best-fit relations measured using the biweight estimator (Beers et al. 1990) and a fixed slope of −0.085. The dashed lines correspond to ±3 σ from the best-fit line, where σ is the dispersion of the objects used for the fit (~0.1 in all four clusters). The thin solid lines correspond to the 3 σ and 5 σ detection limits in $V - I$ color. The open circles represent galaxies retained as cluster members after using their photometric redshifts and a particular Monte Carlo realization of the statistical subtraction. The filled circles are spectroscopically confirmed members with absorption-line spectra, while the crosses represent spectroscopically confirmed members with emission-line spectra. The filled squares and diamonds represent two families of models (see text for details). Spectroscopic redshifts are used in membership determination, where available. The solid histogram in each panel represents the number of objects within 3 σ from the best-fit red sequence after averaging over 100 Monte Carlo realizations of the statistical subtraction.
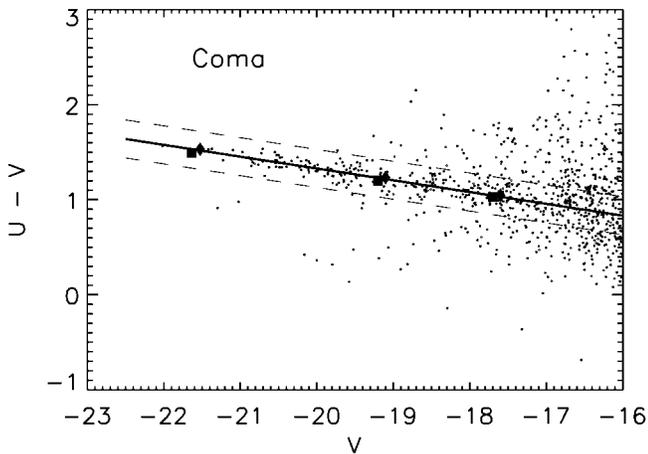
Fig. 2.—CMR of Coma for all the galaxies in the catalog by Terlevich et al. (2001). Observed magnitudes are converted to absolute magnitudes using the distance modulus of Coma (35.16), and observed colors are converted to rest-frame colors using tabulated K-corrections (Poggianti 1997). The solid and dashed lines and the filled circles, squares, and diamonds have the same meaning as in Fig. 1.

5. THE TRUNCATION OF THE RED SEQUENCE

Perhaps the most interesting result of our analysis is that the red sequence in our clusters is well populated at magnitudes brighter than ~22 but is unusually "empty" at fainter magnitudes. The histograms in Figure 1 show the number of cluster members within ~3 σ from the best-fit relation, after averaging over 100 Monte Carlo realizations of the statistical subtraction. The paucity of low-luminosity red galaxies at high z occurs at magnitudes well above our completeness limit and in all the clusters under investigation. There is no clear evidence for such a deficiency in Cl 1040.7−1155 ($z = 0.7$), but given its very low fraction of objects with absorption-line spectra, it cannot be ruled out statistically either.

In order to quantify this effect, we combine the histograms shown in Figure 1, correcting colors and magnitudes to a common redshift of 0.75. The result is shown in Figure 3a. Figure 3b shows the corresponding result for the Coma Cluster. For the high-z clusters, nonmembers have been excluded as described in § 3. The dashed histogram shows the corresponding result when membership is based solely on photometric redshifts. In Coma, membership information is available from spectroscopy for a large number of galaxies, and we have corrected the number of red galaxies in each magnitude bin for background and foreground contamination using a redshift catalog kindly provided by M. Colless and the same procedure as in Mobasher et al. (2003).

The histogram of the EDisCS clusters shows a decrease in the number of $\lesssim 0.4L_*$ red-sequence galaxies. This effect is present in all our clusters individually, with the possible exception of Cl 1040.7−1155, as discussed above. Indeed, the "luminosity function" of the red galaxies in these clusters shows the same decrease despite the variety in cluster properties such as velocity dispersion, richness, concentration, and substructure (S. D. M. White et al. 2004, in preparation; C. Halliday et al. 2004, in preparation). Unfortunately, such a deficiency coincides with the well-known "dip" in the luminosity function of the Coma Cluster (Godwin & Peach 1977). However, the behavior of the Coma Cluster seems quite "untypical." De Propris et al. (2003a), for example, have shown that the luminosity
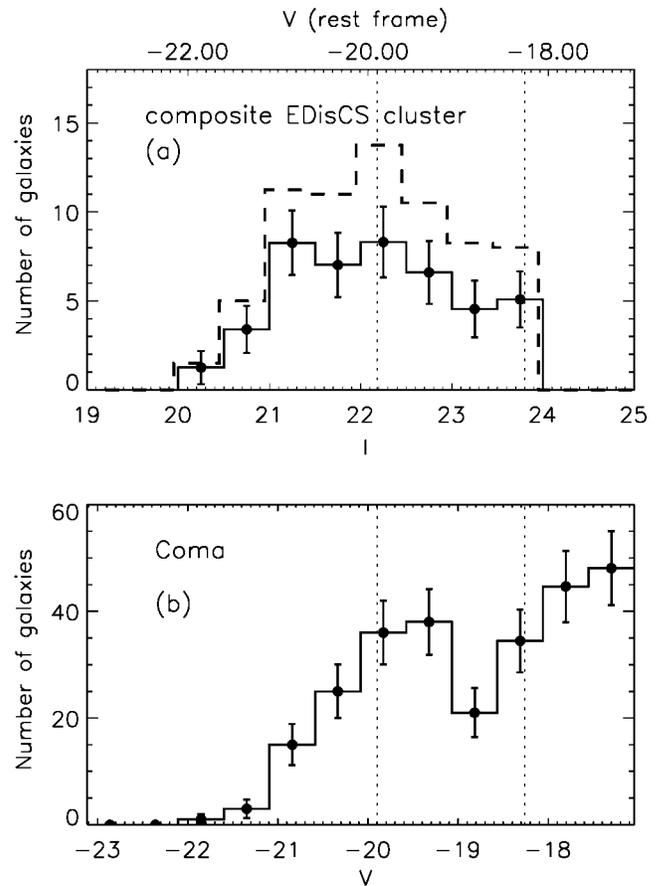
Fig. 3.—Average number of galaxies on the red sequence as a function of magnitude for our composite cluster at redshift 0.75 (panel a) and the Coma cluster (panel b). Error bars represent Poisson errors. The scale on the top of panel a shows the rest-frame V-band magnitude corresponding to the observed I-band magnitudes after correcting for passive evolution between $z = 0.75$ and $z = 0$. The dashed histogram in panel a is obtained when membership is based solely on photometric redshifts and when no statistical correction is applied. A small shift in the x-coordinate has been applied to make the plot more easily readable.

function of early (passive) spectral types increases going to fainter magnitudes in clusters in the Two-Degree Field (2dF) survey.

After correcting for passive evolution with the single-burst model shown in Figures 1 and 2, the histograms shown in Figure 3 are significantly different. A Kolmogorov-Smirnov test rejects the hypothesis that the two histograms are drawn from the same parent distribution at the ~95% level. Our correction for passive evolution is ~0.8 mag at V from $z = 0$ to $z = 0.75$ and is consistent with studies of the fundamental plane (Wuyts et al. 2004). An increase in this correction by 0.2 mag or more lowers the significance of the effect to ~80%.

If we arbitrarily classify as "luminous" galaxies those brighter than $M_V = -19.9$ (this corresponds to an observed I-band magnitude of 22.18 at redshift 0.75), and as "faint" those galaxies that are fainter than this magnitude and brighter than -18.36 (this corresponds to the limiting magnitude in the I band for which all the selected objects are above the 5 σ detection limit in the V band), we obtain a luminous-to-faint ratio for the Coma Cluster of 0.34 ± 0.06 (the error has been estimated assuming Poisson statistics and, for the EDisCS clusters, includes the error associated with the statistical field sub-

traction). The corresponding value of the luminous-to-faint ratio for the composite EDisCS cluster is equal to 0.81 ± 0.18. Therefore, for the composite high-redshift cluster and the Coma Cluster, the difference between their respective ratios is at about the 3 σ level.

The results are robust against both the technique adopted for removing noncluster members and the photometric errors. The red galaxy deficit is also detected when rejecting nonmembers using a purely statistical subtraction or a more stringent criterion for membership based solely on photometric redshifts. In fact, a deficit is also evident in the *full* photometric catalog, when no field correction is attempted. Photometric errors in the EDisCS catalog are comparable to the errors in the Terlevich et al. data; therefore, the differences observed in the distributions of Figure 3 cannot be a spurious result arising from photometric errors. As a further test, we performed a series of Monte Carlo realizations (100) whereby each point in the Coma histogram was scattered around the CMR taking into account the typical error on color and magnitude. The shape of the histogram is not found to vary significantly.

6. DISCUSSION

A decline in the number of red-sequence members at faint magnitudes was first observed in clusters at $z = 0.25$ by Smail et al. (1998). Evidence for a "truncation" of the red sequence has been noticed in a cluster at $z = 1.2$ by Kajisawa et al. (2000) and Nakata et al. (2001). There have, however, been speculations from the same authors that such a result was spurious because of limited area coverage (<0.33 Mpc) and strong luminosity segregation (see the discussion by Kodama et al.

2004, who obtain a similar result for early-type galaxies in a single deep field).

The CMRs of the EDisCS clusters at $z \sim 0.8$ show a deficiency of red, relatively faint galaxies and suggest that such a deficit may be a universal phenomenon in clusters at these redshifts. Our investigation shows that a large fraction of present-day passive $\lesssim 0.4L_*$ galaxies must have moved on to the CMR at redshifts lower than 0.8. Their SF activity therefore must have ended after $z \sim 0.8$. The physical mechanisms and the characteristic timescales of this transformation are not yet understood. The populations of blue galaxies observed in distant clusters are the logical progenitors for a significant fraction of the faint red galaxies at $z = 0$ (Smail et al. 1998; Kodama & Bower 2001; De Propris et al. 2003b).

It is clear that a formation scenario, in which all red galaxies in clusters evolved passively after a synchronous monolithic collapse at $z \gtrsim 2$–3, is inconsistent with observations. Our results indicate that present-day passive galaxies follow different evolutionary paths, depending on their luminosity. Future studies, including the intermediate-redshift clusters in the EDisCS sample, will help us to understand the relative importance of star formation and metallicity in establishing the observed red sequence.

REFERENCES

Beers, T. C., Flynn, K., & Gebhardt, K. 1990, AJ, 100, 32
Bertin, E., & Arnouts, S. 1996, A&AS, 117, 393
Bolzonella, M., Miralles, J.-M., & Pelló, R. 2000, A&A, 363, 476
Brunner, R. J., & Lubin, L. M. 2000, AJ, 120, 2851
Bruzual, G., & Charlot, S. 2003, MNRAS, 344, 1000
De Lucia, G., Kauffmann, G., & White, S. D. M. 2004, MNRAS, 349, 1101
De Propris, R., Colless, M., & Driver, S. P. 2003a, MNRAS, 342, 725
De Propris, R., Eisenhardt, P. R., Stanford, S. A., & Dickinson, M. 1998, ApJ, 503, L45
De Propris, R., Stanford, S. A., Eisenhardt, P. R., & Dickinson, M. 2003b, ApJ, 598, 20
Dressler, A., Smail, I., Poggianti, B. M., Butcher, H., Couch, W. J., Ellis, R. S., & Oemler, A., Jr. 1999, ApJS, 122, 51
Ellis, R. S., Smail, I., Dressler, A., Couch, W. J., Oemler, A., Jr., Butcher, H., & Sharples, R. M. 1997, ApJ, 483, 582
Gladders, M. D., López-Cruz, O., Yee, H. K. C., & Kodama, T. 1998, ApJ, 501, 571
Godwin, J. G., & Peach, J. V. 1977, MNRAS, 181, 323
Kajisawa, M., et al. 2000, PASJ, 52, 61
Kauffmann, G., & Charlot, S. 1998, MNRAS, 294, 705

Kodama, T., Arimoto, N., Barger, A. J., & Aragón-Salamanca, A. 1998, A&A, 334, 99
Kodama, T., & Bower, R. G. 2001, MNRAS, 321, 18
Kodama, T., et al. 2004, MNRAS, 350, 1005
Mobasher, B., et al. 2003, ApJ, 587, 605
Nakata, F., et al. 2001, PASJ, 53, 1139
Poggianti, B. M. 1997, A&AS, 122, 399
Poggianti, B. M., et al. 2001, ApJ, 562, 689
Poggianti, B. M., Smail, I., Dressler, A., Couch, W. J., Barger, A. J., Butcher, H., Ellis, R. S., & Oemler, A., Jr. 1999, ApJ, 518, 576
Rudnick, G., et al. 2001, AJ, 122, 2205
———. 2003, Messenger, 112, 19
Smail, I., Edge, A. C., Ellis, R. S., & Blandford, R. D. 1998, MNRAS, 293, 124
Stanford, S. A., Eisenhardt, P. R., & Dickinson, M. 1998, ApJ, 492, 461
Terlevich, A. I., Caldwell, N., & Bower, R. G. 2001, MNRAS, 326, 1547
van Dokkum, P. G., & Franx, M. 1996, MNRAS, 281, 985
Visvanathan, N., & Sandage, A. 1977, ApJ, 216, 214
Wuyts, S., van Dokkum, P. G., Kelson, D. D., Franx, M., & Illingworth, G. D. 2004, ApJ, 605, 677